Steel and Composite Structures, *Vol. 22, No. 5 (2016) 1019-1038*
DOI: http://dx.doi.org/10.12989/scs.2016.22.5.1019

Effect of high-strength concrete on shear behavior of dry joints in precast concrete segmental bridges

Haibo Jiang [1a], Ying Chen [1], Airong Liu [*2], Tianlong Wang [1] and Zhuangcheng Fang [1]

[1] *School of Civil and Transportation Engineering, Guangdong University of Technology, Guangzhou Higher Education Mega Center, Guangzhou, China*
[2] *Guangzhou University-Tamkang University Joint Research Center for Engineering Structure Disaster Prevention and Control, Guangzhou University, Guangzhou Higher Education Mega Center, Guangzhou, China*

(*Received June 16, 2016, Revised November 02, 2016, Accepted November 09, 2016*)

Abstract. The use of high-strength concrete (HSC) in precast concrete segmental bridges (PCSBs) can minimize the superstructure geometry and reduce beam weight, which can accelerate the construction speed. Dry joints between the segments in PCSBs introduce discontinuity and require special attention in design and construction. Cracks in dry joints initiate more easily than those in epoxy joints in construction period or in service. Due to the higher rupture strength of HSC, the higher cracking resistance can be achieved. In this study, shear behavior of dry joints in PCSBs was investigated by experiments, especially focusing on cracking resistance and shear strength of HSC dry joints. It can be concluded that the use of HSC can improve the cracking resistance, shear strength, and ductility of monolithic, single-keyed and three-keyed specimens. The experimental results obtained from tests were compared with the AASHTO 2003 design provisions. The AASHTO 2003 provision underestimates the shear capacity of single-keyed dry joint C50 and C70 HSC specimens, underestimates the shear strength of three-keyed dry joint C70 HSC specimens, and overestimates the shear capacity of three-keyed dry joint C50 HSC specimens.

Keywords: dry joint; high-strength concrete (HSC); precast concrete segmental bridges (PCSBs); shear strength

1. Introduction

High-strength concrete (HSC) has cube concrete strength in the range of 50-80 MPa, according to the Chinese code of technical specification for high-strength concrete structures (High strength and high performance concrete committee of Chinese Society of Civil Engineering 1999). As a matter of fact, HSC is characterized by increased modulus of elasticity, chemical resistance, freeze thaw resistance, lower creep, lower drying shrinkage and lower permeability. In recent years, HSC is increasingly in civil engineering practice due to its higher strength and better durability with respect to normal strength concrete. Furthermore HSC can be used to lower production cost decreasing member size or increasing structural member spacing, which is especially suitable for

*Corresponding author, Professor, E-mail: Liuar@gzhu.edu.cn
[a] Professor, E-mail: hbjiang@gdut.edu.cn

http://www.techno-press.org/?journal=scs&subpage=6 ISSN: 1229-9367 (Print), 1598-6233 (Online)

precast concrete segmental bridges (PCSBs).

A large number of researches have been carried out to investigate the structural behavior of prestressed HSC beam. French *et al*. (1998) conducted a parametric study to determine the viability of using HSC in prestressed bridge girders. Two long span prestressed bridge girders were constructed to investigate transfer lengths, prestress losses, fatigue performance, shear and ultimate strength of girders cast with HSC. Teoh *et al*. (1999) carried out tests to investigate nine prototype pretensioned HSC I-beams to measure the maximum shear strengths. The major parameters included the compressive strength of the concrete and the amount of prestressing force. It was found that the maximum shear strength is closely proportional to the square root of the compressive strength of the concrete, while the effect of prestressing force is insignificant. Li and Zhao (2003) made the conclusion that with the further study and application of HSC, it is an irresistible trend to employ HSC to the bridges. The advantage of continuous beams has been acknowledged on the bridge. With the development of prestress, the technology of external prestress has shown good prospects, so the combination of the three technologies can ensure excellent economic and social benefits. Nagle and Kuchma (2007) conducted a series of eighteen shear-friction tests and twenty beam shear tests, with the aim of generating the experimental data that were needed for the extension of the American Association of State Highway and Transportation Officials load and resistance factor design (AASHTO LRFD) bridge design specifications to HSC. The results of the shear-friction tests indicate that the experimentally measured resistance is typically larger than that used in the derivation of the LRFD shear provisions. Al-Omaishi *et al*. (2009) conducted research for estimating prestress losses in pretensioned HSC bridge girders, and summarized the portion of that work on concrete properties that have an impact on design for long-term effects: modulus of elasticity, shrinkage, and creep. The research findings were adopted into the 2005 and 2006 interim provisions of the AASHTO LRFD specifications. Campione *et al*. (2014) established a model for the prediction of flexural and shear resistance of HSC beams with longitudinal bars and stirrups, based on the evaluation of the resistance contribution due to beam and arch actions including bond splitting and concrete crushing failure modes. It was shown that the model satisfactorily fitted the experimental results. Shi and Liu (2014) established the shearing strength formula of high strength concrete beams under concentrated load, based on the previous results on the experimental study of shear performance of HSC beam and the application of mathematical statistics theory. The ultimate strength calculated by regression analysis matched with the experimental results well.

Nowadays, with superior durability, low life cycle costs and quality control readily achieved, segmental bridges are favourable alternatives for long spans and for construction in areas where minimal disruption of the environment is required. Due to the simplicity of construction of precast segmental girders with dry joints, dry joints are still opted in many occasions because the technique does not need the usage of epoxy and temporary prestress. Though the performance of the dry joints in segmental construction is highly influenced by environmental factors, it reduces the time and cost of the construction.

Many studies have been conducted on the mechanical behavior of precast conventional concrete segmental bridges with dry joints or epoxied joints since the 1950s (Jones 1959, Gaston and Kriz 1964, Diaz 1975, Koseki and Breen 1983, Bakhoum 1990, Leung *et al*. 1994, Turmo *et al*. 2006, Li *et al*. 2013, Saibabu *et al*. 2013, Jiang *et al*. 2016, Shin and Chung *et al*. 2016). From these tests, it shows that the shear strength of segments joined with epoxy is similar to that of monolithically cast segments, but their failure is brittle. Dry joints with single or multiple keys develop a strength lower than that of epoxied joints.

The tests on shear behavior of dry joints in PCSBs are carried out by several researchers. Buyukozturk *et al*. (1990) concluded that the strength of epoxied joints was consistently higher than that of dry joints and the failure of the epoxied joints was very sudden and brittle, based on a series of single-keyed dry or epoxy joint tests. Formulas were proposed for assessing the shear strength of PCSB epoxied or dry joints.

Zhou *et al*. (2005) found out that AASHTO 2003 and other design criteria tended to underestimate the shear strength of single-keyed joints and three-keyed epoxied joints, and overestimate the shear capacity of three-keyed dry joints.

Issa and Abdalla (2007) undertook a group of five full-depth male-female shear key specimens tests with the objective of examining the shear capacity of single-keyed epoxied joints. Comparing with the cold-weather epoxy specimens, the hot-weather epoxy specimens showed an increase of approximately 28% in shear capacity. The fatigue and water tightness at a segment joint of a segmental construction bridge deck system were also tested.

Jiang *et al*. (2015) tested a group of full-scale dry joints with castellated keys specimens under different confining stress levels. Two crack modes for the single-keyed joints were explicitly proposed. The phenomenon of sequential failure of three-keyed dry joints from the inferior key to the superior one was observed in the tests and verified by finite-element simulation. This conclusion could be extended to the shear strength of three-keyed dry joints to improve the formula.

In addition, there were various finite element models on shear keys reported, in order to analyze the shear behavior of keyed joints under shear loading (notably Turmo *et al*. 2012, Alcalde *et al*. 2013, Shamass *et al*. 2015, 2016).

To achieve the most rapid construction speed, HSC can be used in PCSBs due to lessen geometry and self-weight. HSC can also suppress cracking initiation and enhance the cracking resistance of dry joints. Although Buyukozturk (1990), Zhou (2005), Issa and Abdalla (2007), and other researchers studied on the shear behavior of dry joints with the compressive strength of concrete varied from 30 MPa to 50 MPa in most of the cases, there are very limited experimental studies on the shear behavior of dry joints with the compressive strength of concrete of more than 50 MPa. The widespread use of HSC has made it necessary to review dry joints in PCSBs design codes and specifications for their applicability to HSC.

2. Research objectives

In this study, an experimental program has been carried out to investigate the shear behavior of monolithic, single-keyed, and three-keyed specimens of C50 and C70 HSC under static load. The geometry size of the keyed dry joints is similar to that of Wuhu No. 2 Yangtze River Bridge in Anhui province of China. The cracking resistance, shear strength and residual strength of single-keyed and three-keyed dry joints in PCSBs of C70 HSC have not been researched specially in literature, which is very important for design and construction. The effect of concrete strength in HSC scope on shear behavior, such as cracking resistance, shear strength, residual strength, normalized ultimate shear stress and ductility, has seldom reported to author's knowledge. The experimental cases about three-keyed dry joints specimens of HSC have scarcely been documented. This study can highlight the precious aspects of dry joints in PCSBs. The test results in this paper can broaden the experimental database of dry joint specimens and be used for verifying the relevant design codes.

3. Experimental program

3.1 Test specimens

Push-off specimens similar to those used by other researchers (Buyukozturk *et al*. 1990, Zhou *et al*. 2005, and Jiang *et al*. 2015) were adopted to study the shear behavior of dry joints. Figs. 1-2 show monolithic, single-keyed dry joint and three-keyed dry joint specimens of HSC used for the

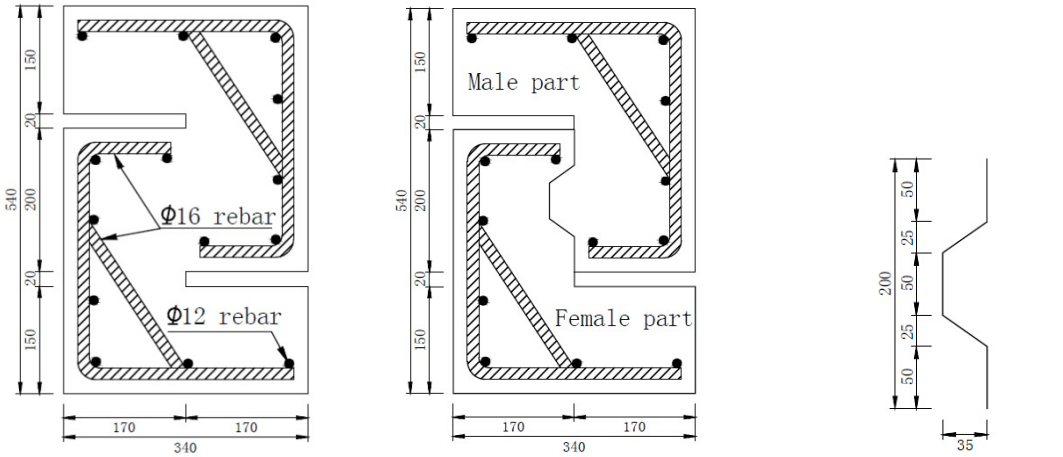

(a) Monolithic joint (b) Single-keyed dry joint (c) Detail of single-key

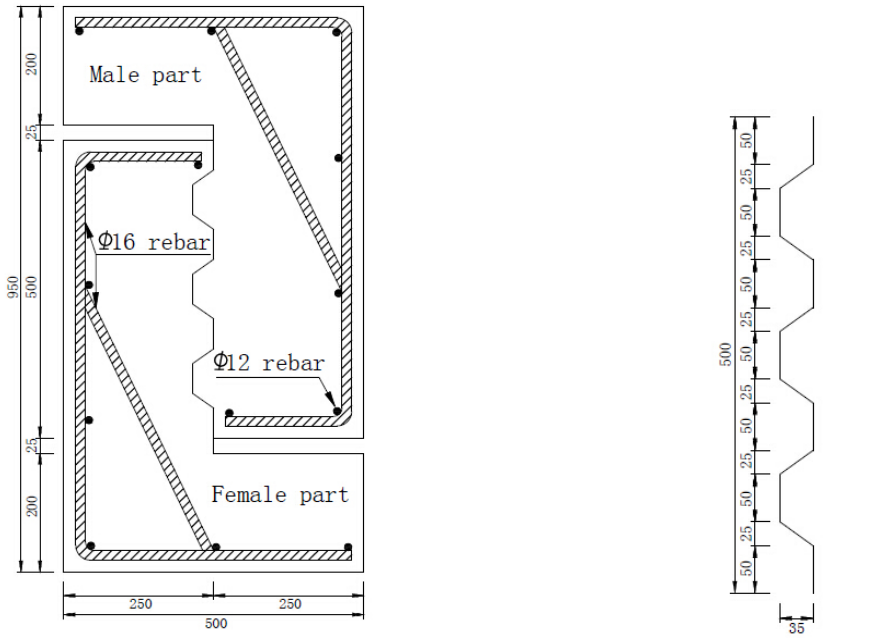

(d) Three-keyed dry joint (e) Detail of three-keys

Fig. 1 Specimen dimensions and configurations for test specimens (mm)


Fig. 2 Picture of testing specimens

Table 1 Summary of experimental parameters

Sequence number	Specimen	Type of joints	Strength grade (MPa)	Confining Stress (MPa)	Specimen amount
1	M0-H5-0.5	Monolithic joint	C50	0.5	2
2	M0-H5-1.0	Monolithic joint	C50	1.0	2
3	M0-H5-2.0	Monolithic joint	C50	2.0	2
4	M0-H7-0.5	Monolithic joint	C70	0.5	2
5	M0-H7-1.0	Monolithic joint	C70	1.0	2
6	M0-H7-2.0	Monolithic joint	C70	2.0	2
7	K1-H5-0.5	Single-keyed joint	C50	0.5	2
8	K1-H5-1.0	Single-keyed joint	C50	1.0	2
9	K1-H5-2.0	Single-keyed joint	C50	2.0	2
10	K1-H7-0.5	Single-keyed joint	C70	0.5	2
11	K1-H7-1.0	Single-keyed joint	C70	1.0	2
12	K1-H7-2.0	Single-keyed joint	C70	2.0	2
13	K3-H5-0.5	Three-keyed joint	C50	0.5	2
14	K3-H5-1.0	Three-keyed joint	C50	1.0	2
15	K3-H5-2.0	Three-keyed joint	C50	2.0	2
16	K3-H7-0.5	Three-keyed joint	C70	0.5	2
17	K3-H7-1.0	Three-keyed joint	C70	1.0	2
18	K3-H7-2.0	Three-keyed joint	C70	2.0	2

Table 2 Concrete mix proportions

Strength grade	Ratio of water to cement	Cement (kg/m^3)	Fine aggregate (kg/m^3)	Coarse aggregate (kg/m^3)	Water (kg/m^3)	Superplasticizer (kg/m^3)
C50	0.44	418	719	1125	184	——
C70	0.33	447	703	1147	148	4.43

Note: Coarse aggregate range in size from 5 mm to 15 mm

tests. All the specimens have a thickness of 100 mm whose size effect of thickness has been neglected in this study. 12 mm and 16 mm diameter rebars were used in the specimens to prevent the concrete failure prior to the failure of keys. In the tests, the main parameters adopted for the investigation were joint types (monolithic joints or keyed dry joints), concrete strength (C50 or C70 HSC), key numbers (single key or three keys), and confining stress levels (0.5 MPa, 1.0 MPa, and 2.0 MPa) as listed in Table 1.

3.2 Materials

Two concrete mix proportions are list in Table 2. The two mixtures of C50 and C70 HSC were designed with an expected compressive strength of 50 MPa and 70 MPa respectively after 28 days based on tests of 15 cm cubic specimens according to JTG D62-2004 (2004). The mix constituents of C50 and C70 HSC both include P·I 42.5 cement, coarse and fine aggregates and water, but C70 adds superplasticizer. Water to cementitious material ratio of C50 and C70 is 0.44 and 0.33 respectively. C50 and C70 HSC was elaborated at the laboratory by a horizontal forced-action mixer of 350 L capacity. In order to prevent the failure of female parts prior to that of male parts, the female parts of keyed joint specimens were cast a week earlier than the male parts intentionally. The cylinder concrete strength of female parts of keyed joint specimens was higher than that of male parts by designing. Actual concrete strength values of monolithic specimens and dry joints specimens can be found in Table 3.

The results of all specimens are documented in Table 3. The specimen nomenclature system shown in Table 3 comprises of four groups of characters or numbers. The first character in first group can be

M = monolithic specimens, and K = keyed joint specimens. The number following it represents the number of keys, e.g., "0" = no key, "1" = one key, and "3" = three keys. The second group gives the expected concrete strength of monolithic specimens and keyed joint specimens, e.g., H5 represents C50 HSC, and H7 identifies the C70 HSC. The number in the third group indicates the confining pressure ("0.5" = 0.5 MPa, "1.0" = 1.0 MPa, and "2.0" = 2.0 MPa). The last group including only one character is to distinguish two same specimens (for instance, *a* = the first one, and *b* = the second one).

3.3 Testing setup and instrumentation

The confining pressure, simulating the effect of prestressing in segmental bridges, was applied using a confining grid and a hydraulic pump. The confining grid consists of two double I16 sections, and two 35 mm diameter steel rods. The confinement pressure was calculated as the ratio between force in the jack and the joint's area. The confining pressure was applied by a jack, powered by a hydraulic pump, and was measured by using pressure sensors and force monitor before the hydraulic jack was set up. A layer of sliding plastic plate was placed at one side of the concrete surface of the specimens and a steel hinge was also arranged before the steel form to eliminate the vertical friction forces from the steel form. Two LVDTs (linear variable differential transducer) were mounted on one side of the specimens to observe the relative vertical slippage, and one LVDT was employed for horizontal dilation. The displacement-control tests for all specimens were conducted at a constant stroke rate of 0.1 mm/min. Data acquired during the tests included the applied forces measured by a calibrated internal load cell, horizontal confinement pressure recorded by pressure sensors, vertical slippages through two LVDTs, horizontal dilation

Table 3 Summary of experimental results

Specimens	Male part		Female part		Cracking load V_{cr}	Ultimate load V_u	Residual load	V_{cr}/V_u	Ultimate shear stress A	Normalized ultimate shear stress B	Shear strength by AASHTO V_a	V_u/V_a	Ultimate vertical slippages d_v	Ultimate horizontal dilations d_h
	Cube Concrete strength f_{cu}	Cylinder Concrete strength f'_c	Cube Concrete strength f_{cu}	Cylinder concrete strength f'_c										
	(MPa)	(MPa)	(MPa)	(MPa)	(kN)	(kN)	(kN)		(MPa)	($MPa^{1/2}$)	(kN)		(mm)	(mm)
M0-H5-0.5-a	58.1	52.9	-	-	-	163.1	55.7	-	8.155	1.121	-	-	0.202	0.090
M0-H5-0.5-b	58.1	52.9	-	-	-	177.8	51.1	-	8.890	1.222	-	-	0.181	0.052
M0-H5-1.0-a	58.1	52.9	-	-	-	188.9	66.7	-	9.445	1.299	-	-	0.184	0.315
M0-H5-1.0-b	58.1	52.9	-	-	-	182.4	59.4	-	9.120	1.254	-	-	0.121	0.067
M0-H5-2.0-a	58.1	52.9	-	-	-	194.2	96.7	-	9.710	1.335	-	-	0.523	0.428
M0-H5-2.0-b	58.1	52.9	-	-	-	201.4	86.0	-	10.070	1.385	-	-	0.155	0.020
M0-H7-0.5-a	73.6	60.0	-	-	-	206.9	45.3	-	10.345	1.336	-	-	0.405	0.128
M0-H7-0.5-b	73.6	60.0	-	-	-	202.5	44.2	-	10.125	1.307	-	-	0.465	0.331
M0-H7-1.0-a	73.6	60.0	-	-	-	247.4	49.1	-	12.370	1.597	-	-	0.326	0.023
M0-H7-1.0-b	73.6	60.0	-	-	-	241.5	52.5	-	12.075	1.559	-	-	0.378	0.213
M0-H7-2.0-a	73.6	60.0	-	-	-	278.3	74.3	-	13.915	1.796	-	-	0.226	0.282
M0-H7-2.0-b	73.6	60.0	-	-	-	268.9	84.2	-	13.445	1.736	-	-	0.154	0.063
K1-H5-0.5-a	59.9	54.1	61.3	56.0	63.9	90.3	32.5	0.707	4.517	0.614	83.2	1.085	0.301	0.165
K1-H5-0.5-b	59.9	54.1	61.3	56.0	59.4	84.3	32.5	0.705	4.215	0.573	83.2	1.013	0.345	0.125
K1-H5-1.0-a	59.9	54.1	61.3	56.0	82.2	122.1	41.1	0.673	6.105	0.830	93.7	1.303	0.680	0.086
K1-H5-1.0-b	59.9	54.1	61.3	56.0	80.2	123.0	47.3	0.652	6.150	0.836	93.7	1.313	0.540	0.245
K1-H5-2.0-a	59.9	54.1	61.3	56.0	113.3	139.2	54.6	0.814	6.960	0.946	114.6	1.215	0.355	0.040

Table 3 Continued

Specimens	Male part		Female part		Cracking load V_{cr}	Ultimate load V_u	Residual load	V_{cr}/V_u	Ultimate shear stress A	Normalized ultimate shear stress B	Shear strength by AASHTO V_a	V_u/V_a	Ultimate vertical slippages d_v	Ultimate horizontal dilations d_h
	Cube Concrete strength f_{cu}	Cylinder Concrete strength f'_c	Cube Concrete strength f_{cu}	Cylinder concrete strength f'_c										
	(MPa)	(MPa)	(MPa)	(MPa)	(kN)	(kN)	(kN)		(MPa)	($MPa^{1/2}$)	(kN)		(mm)	(mm)
K1-H5-2.0-b	59.9	54.1	61.3	56.0	116.1	139.6	59.1	0.832	6.980	0.949	114.6	1.218	0.521	0.115
K1-H7-0.5-a	70.3	60.1	75.0	65.3	81.4	109.8	34.6	0.742	5.490	0.708	87.5	1.255	0.388	0.378
K1-H7-0.5-b	70.3	60.1	75.0	65.3	89.1	101.1	41.8	0.881	5.055	0.652	87.5	1.155	0.288	0.085
K1-H7-1.0-a	70.3	60.1	75.0	65.3	114.7	135.8	40.0	0.845	6.790	0.876	98.4	1.380	0.665	0.730
K1-H7-1.0-b	70.3	60.1	75.0	65.3	111.6	131.6	51.8	0.848	6.580	0.849	98.4	1.337	0.532	0.055
K1-H7-2.0-a	70.3	60.1	75.0	65.3	132.0	149.3	57.7	0.884	7.464	0.963	120.2	1.242	0.364	0.218
K1-H7-2.0-b	70.3	60.1	75.0	65.3	140.3	180.0	66.0	0.779	9.000	1.161	120.2	1.498	0.746	0.275
K3-H5-0.5-a	58.6	54.0	62.6	56.1	155.5	207.6	93.9	0.749	4.152	0.565	246.4	0.843	1.123	0.230
K3-H5-0.5-b	58.6	54.0	62.6	56.1	177.9	227.6	127.6	0.782	4.552	0.619	246.4	0.924	0.830	0.215
K3-H5-1.0-a	58.6	54.0	62.6	56.1	212.4	262.4	123.5	0.809	5.248	0.714	274.8	0.955	0.806	0.403
K3-H5-1.0-b	58.6	54.0	62.6	56.1	185.8	264.1	140.3	0.704	5.282	0.719	274.8	0.961	1.319	0.593
K3-H5-2.0-a	58.6	54.0	62.6	56.1	282.0	326.0	175.0	0.865	6.520	0.887	331.6	0.983	1.185	0.023
K3-H5-2.0-b	58.6	54.0	62.6	56.1	258.8	315.1	174.8	0.821	6.302	0.858	331.6	0.950	1.426	0.408
K3-H7-0.5-a	71.8	61.9	75.0	65.3	191.0	265.2	110.0	0.720	5.304	0.674	263.4	1.007	1.070	1.445
K3-H7-0.5-b	71.8	61.9	75.0	65.3	170.6	278.2	145.2	0.613	5.564	0.707	263.4	1.056	1.121	0.918
K3-H7-1.0-a	71.8	61.9	75.0	65.3	280.7	305.5	126.1	0.919	6.110	0.777	293.4	1.041	0.913	0.268
K3-H7-1.0-b	71.8	61.9	75.0	65.3	262.0	320.2	137.1	0.818	6.404	0.814	293.4	1.091	3.393	1.233
K3-H7-2.0-a	71.8	61.9	75.0	65.3	350.0	393.0	177.9	0.892	7.860	0.999	353.4	1.112	0.980	0.089
K3-H7-2.0-b	71.8	61.9	75.0	65.3	364.1	461.1	174.8	0.789	9.222	1.172	353.4	1.305	1.375	0.335

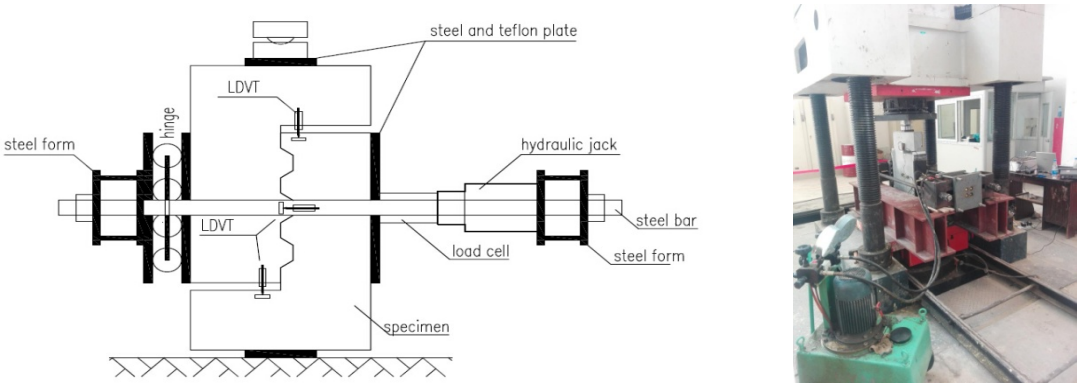

(a) sketch of setup (b) photo of setup

Fig. 3 Typical experimental setup for dry joints

via one LVDT by using a DH3816 data processor. A general sketch of the instrumentation set-up for specimens is showed in Fig. 3.

4. Experimental results

4.1 Observed behavior

Totally twelve specimens of keyed dry joints and six monolithic specimens were tested. Each specimen is generally under a different combination of parameters. The photos of typical failure modes are presented in Fig. 4. The sketches of the cracking sequences and failure modes of monolithic joints and dry joints are depicted in Figs. 5-7. The loads and slips corresponding to pictures of crack initiations, crack propagation, and failure modes are list in captions.

4.1.1 Monolithic joint specimens

Three monolithic specimens of C50 HSC and three monolithic specimens of C70 HSC were tested. For C50 HSC, several nearly vertical cracks initiated at the ultimate load and continuously developed. Shortly after a failure plane was formed, the specimens slid into two parts as shown in Figs. 5(a)-(b). For C70 HSC, several nearly vertical cracks initiated at the ultimate load with a harsh sound and continuously developed. The specimens also slid into two parts as shown in Figs. 5(c)-(d).

4.1.2 Single-keyed dry joint specimens

Three single-keyed dry joint specimens of C50 HSC and three single-keyed dry joint specimens of C70 HSC were tested. The cracking patterns of single-keyed dry joint specimens of C50 HSC were depicted in Figs. 6(a)-(c). The first crack formed at the bottom corner of the single-key and propagated at 61° respective to the horizontal direction. The second crack initiated and developed over the first crack, and then several short diagonal cracks were initiated at the root of the key. After the loads were increased, the cracks interconnected. The upper part of the key was cut off, and the lower part was crushed. The cracking patterns of single-keyed dry joint specimens of C70 HSC were depicted in Figs. 6(d)-(f). The first crack formed at the bottom corner of the single-key

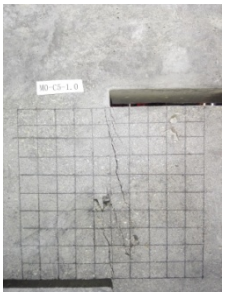

(a) M0-H5-1.0-b (182.4 kN, 0.121 mm)

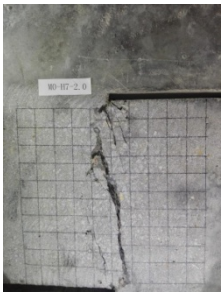

(b) M0-H7-2.0-a (74.3 kN, 2.981 mm)

(c) K1-H5-2.0-b (131.6 kN, 0.532 mm)

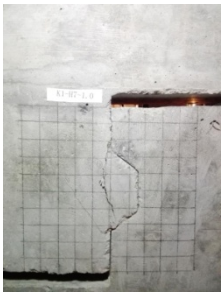

(d) K1-H7-1.0-b (125.8 kN, 0.416 mm)

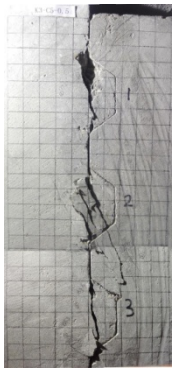

(e) K3-H5-0.5-a (145.4 kN, 1.935 mm)

(f) K3-H7-1.0-a (231.3 kN, 1.875mm)

Fig. 4 Photos of typical crack patterns

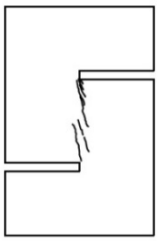

(a) Crack initiation for C50 HSC specimens (182.4 kN, 0.121 mm for M0-H5-1.0-b)

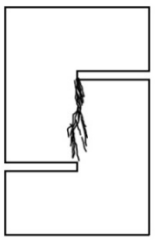

(b) Failure mode for C50 HSC specimens (60.8 kN, 3.720 mm for M0-H5-1.0-b)

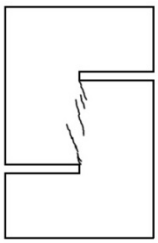

(c) Crack initiation for C70 HSC specimens (278.3 kN, 0.226 mm for M0-H7-2.0-a)

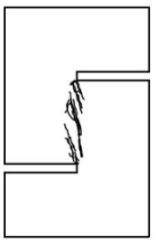

(d) Failure mode for C70 HSC specimens (74.3 kN, 2.981 mm for M0-H7-2.0-a)

Fig. 5 Sketches of cracking patterns of monolithic specimens

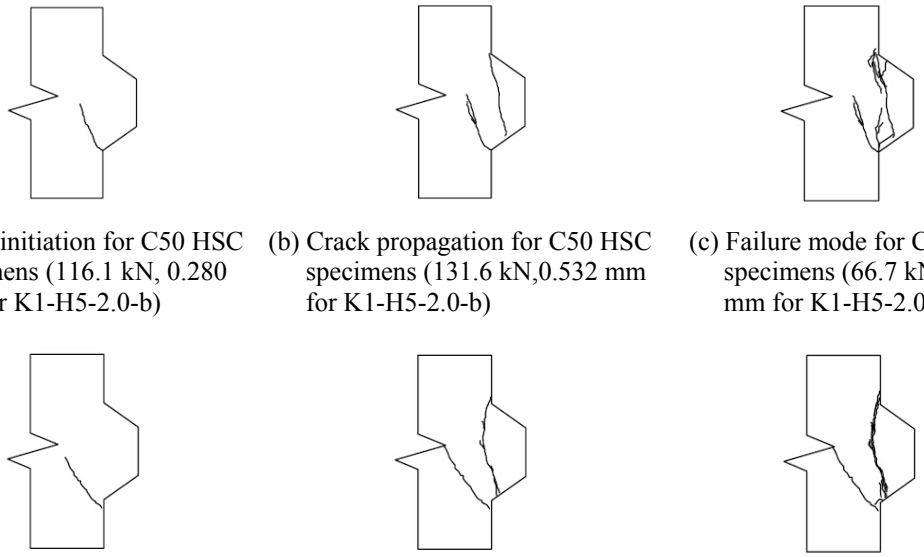

(a) Crack initiation for C50 HSC specimens (116.1 kN, 0.280 mm for K1-H5-2.0-b)

(b) Crack propagation for C50 HSC specimens (131.6 kN,0.532 mm for K1-H5-2.0-b)

(c) Failure mode for C50 HSC specimens (66.7 kN, 0.795 mm for K1-H5-2.0-b)

(d) Crack initiation for C70 HSC specimens (111.6 kN, 0.324 mm for K1-H7-1.0-b)

(e) Crack propagation for C70 HSC specimens (125.8 kN,0.416 mm for K1-H7-1.0-b)

(f) Failure mode for C70 HSC specimens (51.1 kN, 2.759 mm for K1-H7-1.0-b)

Fig. 6 Sketches of cracking patterns of single-keyed dry joint specimens

and propagated at 54° respective to the horizontal direction. Then, a principal vertical crack was initiated at the root of the key. After the loads were increased, the cracks interconnected. The key finally was sheared off.

4.1.3 Three-keyed dry joint specimens

Three specimens of three-keyed dry joints of C50 HSC and three specimens of three-keyed dry joints of C70 HSC were tested. For three-keyed dry joint specimens of C50 HSC, the crack initiated at the bottom corner in the lower key and propagated at 46° respective to the horizontal direction, and then the similar cracks occurred in the other two keys. With load increasing, the cracks propagated upward and eventually the keys were sheared off. The failure sequence that the lower key first failed, followed the upper and the middle one, is shown in Figs. 7(a)-(c). For three-keyed dry joint specimens of C70 HSC, the cracking patterns are resembled with those specimens of C50 HSC. The failure sequence of the keys is from the lower key to the upper and middle keys as shown in Figs. 7(d)-(f).

4.2 Normalized shear stress-slip curves

Typical normalized shear stress-relative vertical displacement curves (shear stress-slip curves) for monolithic joints, single-keyed dry joints, and three-keyed dry joints with confining stress of 0.5 MPa, 1.0 MPa, and 2.0 MPa are shown in Fig. 8. Data are presented graphically on plots where the abscissa gives the values of the vertical relative displacement and the ordinate represents the average normalized shear stress on the joint. The normalized average shear stress is obtained through normalizing the average shear stress with respect to $\sqrt{f_c'}$ of the male part of the

specimens for keyed dry specimens, in order to take into consideration the effect of the variation of cylinder concrete strength in the specimens and make direct correlation with the expression given by AASHTO LRFD (2014) provisions (shear strength of the keyed dry joint is a function of the diagonal-tension cracking load).

The average shear stress is defined as the applied shear force divided by the area of the shear plane (20,000 mm^2 for monolithic joints, and single-keyed joints; and 50,000 mm^2 for three-keyed joints in this study). The shear plane is defined here as the vertical projection of the contact area of two parts of the specimens. For all specimens in Fig. 8, the normalized shear strength increases with the increasing of the confining pressure.

The shear stress-slip curves of the monolithic specimens in Figs. 8(a)-(b) is linear up to a level close to the ultimate load, and shows a sudden drop to approximately horizontal level, which demonstrates a brittle failure mode.

The shear stress-slip curves of the single-keyed dry joint specimens are shown in Figs. 8(c)-(d). It can be seen from the curves of C50 HSC specimens, the load increases linearly with slip up to about 70% of the maximum load, then nonlinearity initiates, and the stiffness of the specimen reduce. After approaching the summit of the plot, the load starts to drop to approximate horizontal level. A similar behavior was observed for C70 HSC specimens.

The shear stress-slip curves of three-keyed dry joint specimens are depicted in Figs. 8(e)-(f).

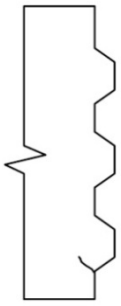

(a) Crack initiation for C50 HSC specimens (155.5 kN, 0.383 mm for K3-H5-0.5-a)

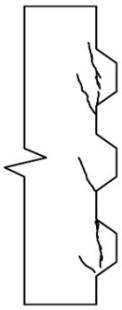

(b) Crack propagation for C50 HSC specimens (187.9 kN, 0.898 mm for K3-H5-0.5-a)

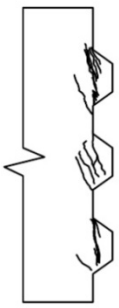

(c) Failure mode for C50 HSC specimens (145.4 kN, 1.935 mm for K3-H5-0.5-a)

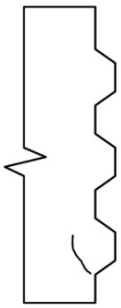

(d) Crack initiation for C70 HSC specimens (350.0 kN, 0.703 mm for K3-H7-2.0-a)

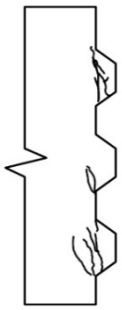

(e) Crack propagation for C70 HSC specimens (392.2 kN, 1.070 mm for K3-H7-2.0-a)

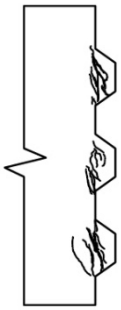

(f) Failure mode for C70 HSC specimens (231.3 kN, 1.875 mm for K3-H7-2.0-a)

Fig. 7 Sketches of cracking patterns of three-keyed dry joint specimens

After the load reaches the maximum value, the curve begins to decrease, and then rises but not more than the maximum value. At last the curve sustains a nearly horizontal level. For C50 HSC specimens, the curve drops gradually and slightly, while for C70 HSC specimens, the value exhibits a certain fluctuation, as the keys failed gradually.

4.3 Cracking load

The cracking loads and ratios of cracking loads to ultimate loads of all specimens are listed in Table 3. For all specimens, the cracking loads increase as the confining pressure increases. However, the confining pressure doesn't influence the ratios of cracking to ultimate loads significantly, because the confining pressure also changes the ultimate loads simultaneously. For single-keyed and three-keyed dry joint specimens, the cracking load of C70 HSC specimen is higher than that of C50 HSC specimen correspondingly, which can infer that higher concrete strength can delay the occurrence of cracking effectively.

4.4 Ultimate load

The ultimate loads of all specimens are listed in Table 3. It can be seen that the increasing of the confining pressure can effectively improve the ultimate loads. In the group of monolithic specimens, the monolithic specimens of C70 HSC with different confining pressures record the highest ultimate loads than those of monolithic specimens of C50 HSC. The ultimate loads of single-keyed dry joint specimens of C70 HSC are less than that of monolithic specimens of C70 HSC. The ultimate load of single-keyed and three-keyed dry joint specimens of C70 HSC are higher than that of single-keyed and three-keyed dry joint specimens of C50 HSC at the same confining pressure, which indicates that concrete strength can improve the ultimate load of single-keyed and three-keyed dry joint specimens.

4.5 Residual load

After the specimen finally was sheared off, the load starts to drop to approximate horizontal level. For monolithic and single-keyed specimens, the residual loads were chosen the shear loads corresponding to the vertical relative slip value (4 mm). For three-keyed specimens, the residual loads were chosen the shear loads corresponding to the vertical relative slip value (6 mm). The residual loads of all specimens are listed in Table 3. For all specimens, the residual loads increase as the confining pressure increases, which can infer that higher confining pressure can improve the residual loads effectively. The residual load of monolithic specimens is higher than that of single-keyed dry joint specimens at the same confining pressure for both C50 and C70 HSC specimens. The reason for this is that after the ultimate load is reached and the joints are fully cracked, the surface roughness of the concrete in the case of monolithically specimens is much higher than the surface roughness for single-keyed joints.

The average residual loads of all specimens are list in Table 4. For C50 and C70 HSC, the standard deviation of the monolithic specimens is 18.2 and 16.8, that of single-keyed dry joint specimens is 11.2 and 11.9, as well as that of three-keyed dry joint specimens is 31.6 and 26.9 respectively. From Table 4, the monolithic specimens of C50 HSC have the higher average residual load than that of monolithic specimens of C70 HSC. For the case of single-keyed dry joint specimens and three-keyed dry joint specimens, it can be found that the higher strength concrete can slightly improve the average residual load. From Table 4, the improvement is 4.1% and 8.6%.

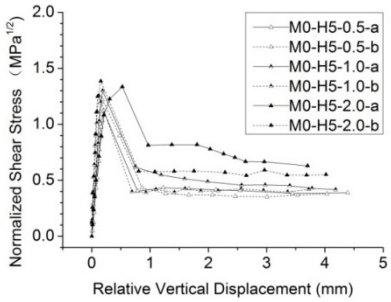

(a) Monolithic specimens of C50 HSC

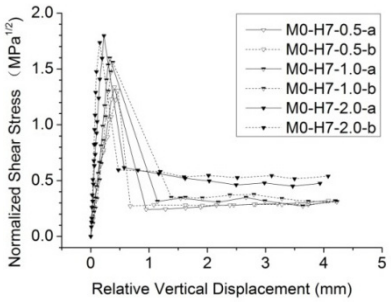

(b) Monolithic specimens of C70 HSC

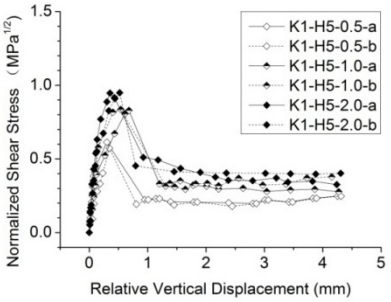

(c) Single-keyed specimens of C50 HSC

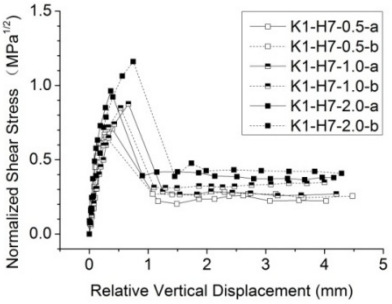

(d) Single-keyed specimens of C70 HSC

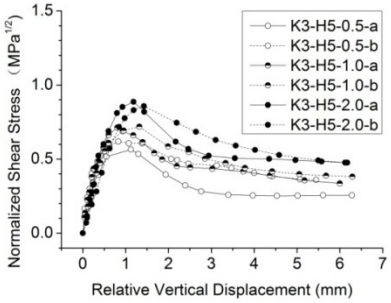

(e) Three-keyed specimens of C50 HSC

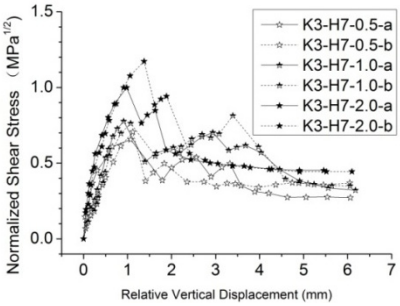

(f) Three-keyed specimens of C70 HSC

Fig. 8 Normalized shear stress relative displacement curves

4.6 Comparison of normalized shear stress

From Table 3, it can be found that the normalized shear stress of all specimens increases with the increasing of confining pressures. The average normalized shear stresses of all specimens are list in Table 4. From Table 4, the monolithic specimens of C70 HSC have the highest average normalized shear strength, as recorded of 1.555. The average normalized shear stress of C50 HSC monolithic specimens rank at the top near that of monolithic specimens of C70 HSC. The average normalized shear strength of three-keyed dry joint specimen of C50 HSC is 8.1% lower than that of single-keyed dry joint specimen of C50 HSC. Meanwhile, the average normalized shear strength of three-keyed dry joint specimens of C70 HSC is 1.3% lower than that of single-keyed dry joint specimens of C70 HSC.

Table 4 The average values of all specimens

Specimens	Average value of normalized shear stress ($MPa^{1/2}$)	Average vertical slippage (mm)	Average horizontal dilation (mm)	Average residual load (kN)
M0-H5	1.269	0.228	0.162	69.3
M0-H7	1.555	0.326	0.173	58.3
K1-H5	0.791	0.457	0.129	44.5
K1-H7	0.868	0.497	0.290	48.7
K3-H5	0.727	1.115	0.312	139.2
K3-H7	0.857	1.475	0.715	145.2

Table 5 Effect of concrete strength

Number	Original specimen	Comparative specimen	Cracking load V_{cr} (%)	Ultimate load V_u (%)	Residual load (%)	Normalized ultimate shear stress (%)
1	M0-H5-0.5	M0-H7-0.5	-	20.09	-16.20	12.80
2	M0-H5-1.0	M0-H7-1.0	-	31.67	-19.43	23.62
3	M0-H5-2.0	M0-H7-2.0	-	38.32	-13.25	29.85
4	K1-H5-0.5	K1-H7-0.5	38.28	20.79	17.54	14.57
5	K1-H5-1.0	K1-H7-1.0	39.35	9.10	3.85	3.54
6	K1-H5-2.0	K1-H7-2.0	18.70	18.11	8.80	12.08
7	K3-H5-0.5	K3-H7-0.5	8.46	24.86	15.21	16.64
8	K3-H5-1.0	K3-H7-1.0	36.29	18.84	-0.23	11.03
9	K3-H5-2.0	K3-H7-2.0	32.05	33.22	0.83	24.41

4.7 The vertical slippages and horizontal dilations at ultimate loads

The vertical slippages and horizontal dilations at ultimate loads are important indexes which measure the ductility of the specimens as listed in Table 3. The average value of the vertical slippage and horizontal dilation for each specimen type are tabulated in Table 4. The average vertical slippages of monolithic specimens range from 0.2~0.4 mm, while the horizontal dilations from 0.1~0.2 mm. The vertical slippages and horizontal dilations of single-keyed dry joint specimens are in the scope of 0.1~0.5 mm. The three-keyed dry joint specimens have the larger vertical slippages from 1.1 to 1.5 mm and horizontal dilations from 0.3 to 0.8 mm than those of monolithic specimens and single-keyed dry joint specimens. It can be inferred that three-keyed dry joint specimens have more ductility than those of single-keyed dry joint.

4.8 Effect of concrete strength

The increased percentages of cracking load, ultimate load, residual load, and normalized ultimate shear stress of all specimens affected by concrete strength are listed in Table 5. For monolithic specimens, as the concrete strength increases, ultimate load and normalized ultimate shear stress increase while residual load decreases. For single-keyed specimens, cracking load, ultimate load, residual load, and normalized ultimate shear stress in the Table 5 increase as the

concrete strength increases. For three-keyed specimens, cracking load, ultimate load, and normalized ultimate shear stress increase with the increasing concrete strength, but the relationship between concrete strength and residual load is obscured.

4.9 Shear capacity of joints compared with AASHTO 2003 provisions

AASHTO 2003 gives the following design formula for estimating the shear capacity of key joints in prestressed concrete segmental bridges (in metric unit)

$$V_j = A_k\sqrt{f_c'}(0.9961 + 0.2048\sigma_n) + 0.6A_{sm}\sigma_n (MN) \tag{1}$$

Where, A_k = base areas of all keys in the failure plane (m^2); f'_c = compressive strength of concrete (MPa); σ_n = normal compressive stress in concrete after allowance for all prestress losses determined at the centroid of the cross section (MPa); and A_{sm} = area of contact between smooth surfaces on the failure plane (m^2).

Shear capacity of joints predicted by Eq. (1), originally proposed by Ramirez *et al*. (1993), is taken as the algebraic summation of the shear contribution from the contacting flat parts between segments and the shear contributions of keys. The shear strength of dry joints with castellated keys comprises two contributions. The first contribution is that the friction resistance arises when two flat and compressed surfaces attempt to slide against each other. This resistance is proportional to the actuating compression and the corresponding proportionality factor, which is the friction coefficient, indicated as 0.6 in Eq. (1) in AASHTO 2003 provisions. The second part considers the support effect of the castellated shear keys. These keys permit shear transfer when they are in contact with each other, behaving like small plain concrete corbels (the small dimensions of the keys do not enable us to place conventional reinforcement). The shear strength of the keys by surface area is called cohesion, which is $12\sqrt{f_c'}$ (English unit) or $0.9961\sqrt{f_c'}$ (Metric unit) in Eq. (1). If compression stresses, σ_n exist, then the keys turn out to be small prestressed concrete corbels, increasing the ultimate shear capacity with compression. The corresponding proportionally factor is called internal friction, which is $0.017\sqrt{f_c'}$ (English unit) or $0.2048\sqrt{f_c'}$ (Metric unit) in Eq. (1).

The measured shear strength from tests of dry joints has been compared with AASHTO 2003 provisions, which are listed in Table 3. The average of V_u / V_a of single-keyed dry joint specimens of C50 HSC is 1.191, and the standard deviation is 0.120. The average of V_u / V_a of single-keyed dry joint specimens of C70 HSC is 1.311, and the standard deviation is 0.121. It can be found that the AASHTO 2003 formula is conservative for evaluation of shear capacity for single-keyed dry joints.

Shamass *et al*. 2016 pointed out that concrete tensile strength has a significant effect on the behavior of keyed joints and recommended to use a concrete tensile strength that is as accurate as possible. Increasing the tensile strength of concrete from 7.5%f_{cm} [the Eurocode 2 (BSI 2004) formula] to 10%f_{cm} (the general assumption of tensile strength of concrete) can increase the shear capacity of the joints and the displacement at the peak load up to 25%, depending on the strength of concrete and confining pressure. The tensile strength suggested by Eurocode 2 (BSI 2004) is about 7-7.5% of the compressive strength of the concretes tested by Buyukozturk *et al*. (1990) and Zhou *et al*. (2005). However, there are several factors influencing the shear strength of single-keyed dry joint, like the geometry of keyed dry joint and confining pressure. The effect of concrete tensile strength on the shear strength of single-keyed dry joint is still uncertain. The explanation

Table 6 Comparison between testing results and AASHTO formula

Specimens		Ultimate load V_u (kN)	Shear strength by AASTHO V_a (kN)	V_u / V_a
Zhou 2005	M1-D-K3-1	446	564	0.791
	M1-D-K3-2	437	560	0.780
	M1-D-K3-3	471	611	0.771
Turmo 2006	PC-JC	385	533	0.722
	SFRC-JC	357	509.3	0.701
Jiang 2015	K2-01	141.8	163.3	0.868
	K2-03	137.39	164.4	0.836
	K2-04	127.04	164.4	0.773
	K3-01	181.3	243.3	0.745
	K3-02	235.64	294.7	0.800
This test	K3-H5-0.5	217.6	246.4	0.883
	K3-H5-1.0	263.3	274.8	0.958
	K3-H5-2.0	320.6	331.6	0.967

Average of V_u / V_a = 0.815, Standard Deviation of V_u / V_a = 0.084

for the underestimation of shear strength of single-keyed dry joint and the effect of concrete tensile strength on the shear strength of single-keyed dry joint need more deep exploring.

The average value of V_u / V_a of three-keyed dry joints of C50 HSC is 0.936 and the standard deviation is 0.049. The average value of V_u / V_a of three-keyed dry joints of C70 HSC is 1.102 and the standard deviation is 0.106. In this test, for the three-keyed dry joints, the AASHTO 2003 formula overestimates the shear capacity of three-keyed dry joints of C50 HSC, while the AASHTO 2003 formula underestimates the shear capacity of three-keyed dry joints of C70 HSC.

The deviation between the tests results and the AASHTO 2003 formula on the multi-keyed dry joints can also be found in other papers (Zhou *et al*. 2005, Turmo *et al*. 2006, Jiang *et al*. 2015), which are listed in Table 6. It can be observed that the average value of V_u / V_a is 0.815 and the standard deviation is 0.084, which indicates that AASHTO 2003 formula overestimates the shear strength of three-keyed dry joints with less than or equal to 50 MPa concrete.

This difference may be explained from the fact that Eq. (1) was derived from the theoretical and experimental work of single-keyed joints. The fixing imperfections and stress concentration in joints increase as key number increases; the higher stress concentration and fixing imperfections mean that the summation of individual shear capacity of keys in two-keyed or three-keyed joints cannot be fully developed. From this experimental work, the keys in three-keyed dry joints do not fail simultaneously while they fail sequentially.

5. Conclusions

A series of tests were undertaken to investigate on the shear behavior of different type joint specimens with various parameter combinations. However, the cracking resistance and shear strength of dry joints of HSC has not been researched specifically. This study offers quantitative data and the fundamental behavioral understanding on the cracking and failure mechanism of

keyed dry joints in HSC. Based on the test results and observations, the following conclusions can be drawn.

- The cracking load, ultimate load and the normalized shear stress of all specimens increase with the increasing confining pressure. Based on the test results of vertical slippage and horizontal dilation, three-keyed dry joint specimens have a higher degree of ductility than single-keyed joint specimens.
- The principal crack appears at the ultimate load for monolithic specimens of HSC, and then propagates up to splitting the specimens into two parts immediately. The crack in the single-keyed dry joint specimens occurs at the bottom corner of the key, several diagonal cracks at the root of the key develop and interconnect leading to failure. The failure of single-keyed dry joint specimens of HSC originates from the split of castellated key. The failure of three-keyed dry joint specimens, however, is caused by the failure of the bottom key first, then the top key, and finally the middle key in that sequence.
- Higher concrete strength in dry joints specimens can effectively enhance the cracking loads, ultimate loads, normalized ultimate shear stress and ductility of monolithic specimens, single-keyed specimens and three-keyed specimens. The residual load increases with the increasing of concrete strength for single-keyed specimens, and decreases for monolithic specimens. The effect of the concrete strength on the residual load of three-keyed specimens is obscured.
- The AASHTO 2003 formula underestimates the shear capacity of single-keyed dry joint specimens of C50 and C70 HSC and underestimates the shear capacity of three-keyed dry joint specimens of C70 HSC. The AASHTO 2003 formula overestimates the shear capacity of three-keyed dry joint specimens of C50 HSC.

Acknowledgments

The research presented was sponsored by Science and Technology grant scheme of Department of Education of Guangdong Province in China (2014KTSCX060), Science and Technology Development Special fund (Basic and Applied Basic Research Branch) of Guangdong Province in China (2016A030313699), Science and Technology Planning Project of Guangdong Province in China (2016B050501004), and National International Scientific and Technological Cooperation Base of Wind Resistance and Structural Safety for Engineering Structures (Guangzhou University).

References

AASHTO (2003), Guide specifications for design and construction of segmental concrete bridges; (2nd Ed.), American Association of State Highway and Transportation Officials, Wanshington D.C., USA, 31 p.

AASHTO (2014), AASHTO LRFD bridge design specifications; (6th Ed.), American Association of State Highway and Transportation Officials, Wanshington D.C., USA.

Alcalde, M., Cifuentes, H. and Medina, F. (2013), "Influence of the number of keys on the shear strength of post-tensioned dry joints", *Mater. Construct.*, **63**(310), 297-307.

Al-Omaishi, N., Tadros, M.K. and Seguirant, S.J. (2009), "Elasticity modulus, shrinkage, and creep of high-strength concrete as adopted by AASHTO", *PCI J.*, **54**(3), 44-63.

Bakhoum, M.M. (1990), "Shear behaviour and design of joints in precast concrete segmental bridges", Ph.D. DissertationL Massachusetts Institute of Technology, Cambridge, MA, USA.

BSI (2004), Eurocode 2: design of concrete structures; Part 1-1: General rules and rules for buildings, British Standards Institution, London, England.

Buyukozturk, O., Bakhoum, M.M. and Bettie, S.M. (1990), "Shear behavior of joints in precast concrete segmental bridges", *J. Struct. Eng.*, **12**(3380), 3380-3401. DOI: 10.1061/(ASCE)0733-9445(1990)116

Campione, G., Monaco, A. and Minafo, G. (2014), "Shear strength of high-strength concrete beams: Modeling and design recommendations", *Eng. Struct.*, **69**, 116-122.

CECS 104-1999 (1999), Technical specification for high-strength concrete structures; Standard Press of China, Beijing, China. [In Chinese]

Diaz, B.E. (1975), "The technique of glueing precast elements of the rio-niteroi bridge", *Mater. Constr. Mater. Struct.*, **8**(1), 43-50.

French, C., Mokhtarzadeh, A., Ahlborn, T. and Leon, R. (1998), "High-strength concrete applications to prestressed bridge girders", *Constr. Build. Mater.*, **12**(2-3), 105-113.

Gaston, J.R. and Kriz, L.B. (1964), "Connections in precast concrete structures-scarf joints", *PCI J.*, **9**(3), 37-59.

Issa, M.A. and Abdalla, H.A. (2007), "Structural behavior of single key joints in precast concrete segmental bridges", *J. Bridge Eng.*, **12**(3), 315-324.

Jiang, H., Chen, L., Ma, Z.J. and Feng, W. (2015), "Shear behavior of dry joints with castellated keys in precast concrete segmental bridges", *J. Bridge Eng.*, 04014062.
DOI: 10.1061/(ASCE)BE.1943-5592.0000649

Jiang, H., Wei, R., Ma, Z.J., Li, Y. and Jing, Y. (2016), "Shear strength of steel-reinforced concrete dry joints in precast segmental bridges", *J. Bridge Eng.*, 04016085.
DOI: 10.1061/(ASCE)BE.1943-5592.0000968

Jones, L.L. (1959), "Shear test on joints between precast post-tensioned units", *Mag. Concr. Res.*, **11**(31), 25-30.

JTG D62-2004 (2004), Code for design of highway reinforced concrete and prestressed concrete bridges and culverts; Standard Press of China, Beijing, China. [In Chinese]

Koseki, K. and Breen, J.E. (1983), "Exploratory study of shear strength of joints for precast segmental bridges", Rresearch Report NO. 248-1; Center for Transportation Research, The University of Texas at Austin, Austin, TX, USA.

Leung, Y.W., Deeprasertwong, K. and Takebayashi, T. (1994), "Full-scale destructive test of a precast segmental box girder bridge with dry joints and external tendons", *Proceedings of the Institution of Civil Engineers*: *Structures and Buildings*, London, England, August.

Li, F.Y. and Zhao, R.D. (2003), "Analysis on the structural behaviors of the continuous beam with external prestress and high strength concrete", *Proceedings of International Conference on Advances in Concrete and Structures*, Xuzhou, China, September.

Li, G., Yang, D. and Lei, Y. (2013), "Combined shear and bending behavior of joints in precast concrete segmental beams with external tendons", *J. Bridge Eng.*, **18**(10), 1042-1052.

Nagle, T.J. and Kuchma, D.A. (2007), "Shear transfer resistance in high-strength concrete girders", *Mag. Concr. Res.*, **59**(8), 611-620.

Ramirez, G., MacGregor, R., Kreger, M.E., Roberts-Wollmann, C. and Breen, J. (1993), "Shear strength of segmental structures", *Proceedings of the Workshop AFPC External Prestressing in Structures*, Saint-Rémy-lès-Chevreuse, France, June.

Saibabu, S., Srinivas, V., Sasmal, S., Lakshmanan, N. and Iyer, N.R. (2013), "Performance evaluation of dry and epoxy jointed segmental prestressed box girders under monotonic and cyclic loading", *Constr. Build. Mater.*, **38**, 931-940.

Shamass, R., Zhou, X. and Alfano, G. (2015), "Finite-element analysis of shear-off failure of keyed dry joints in precast concrete segmental bridges", *J. Bridge Eng.*, 04014084.
DOI: 10.1061/(ASCE)BE.1943-5592.0000669

Shamass, R., Zhou, X. and Wu, Z. (2016), "Numerical analysis of shear-off failure of keyed epoxied joints in precast concrete segmental bridges", *J. Bridge Eng.*, 04016108.
DOI: 10.1061/(ASCE)BE.1943-5592.0000971

Shi, Q.Y. and Liu, L.L. (2014), "Research on the shear strength of high-strength concrete beams with web bars by concentrated load", *Proceedings of the 2nd International Conference on Civil Engineering and Material Engineering 2013*, Wuhan, China, December.

Shin, D., Chung, C., Oh, H., Park, S., Kim, I., Kim, Y., Byun, T. and Kang, M. (2016), "Structural behavior of precast concrete deck with ribbed loop joints in a composite bridge", *Smart Struct. Syst., Int. J.*, **17**(4), 559-576.

Teoh, B.K., Mansur, M.A. and Wee, T.H. (1999), "Maximum shear strength of high strength concrete beams", *Proceedings of the 1st International Conference on Advances in Structural Engineering and Mechanics*, Seoul, South Korea, August.

Turmo, J., Ramos, G. and Aparicio, A.C. (2006), "Shear strength of dry joints of concrete panels with and without steel fibres - Application to precast segmental bridges", *Eng. Struct.*, **28**(1), 23-33.

Turmo, J., Ramos, G. and Aparicio, A.C. (2012), "Towards a model of dry shear keyed joints: modelling of panel tests", *Comput. Concr., Int. J.*, **10**(5), 469-487.

Zhou, X.M., Mickleborough, N. and Li, Z.J. (2005), "Shear strength of joints in precast concrete segmental bridges", *ACI Struct J.*, **102**(1), 3-11.

CC